[POSTER] A Particle Filter Approach to Outdoor Localization using Image-based Rendering

Christian Poglitsch[*]   Clemens Arth[†]   Dieter Schmalstieg[‡]   Jonathan Ventura[§]
Graz University of Technology   University of Colorado Colorado Springs

ABSTRACT

We propose an outdoor localization system using a particle filter. In our approach, a textured, geo-registered model of the outdoor environment is used as a reference to estimate the pose of a smartphone. The device position and the orientation obtained from a Global Positioning System (GPS) receiver and an inertial measurement unit (IMU) are used as a first estimation of the true pose. Then, multiple pose hypotheses are randomly distributed about the GPS/IMU measurement and use to produce renderings of the virtual model. With vision-based methods, the rendered images are compared with the image received from the smartphone, and the matching scores are used to update the particle filter. The outcome of our system improves the camera pose estimate in real time without user assistance.

Index Terms: I.3.7 [Computer Graphics]: Virtual Reality; I.4.8 [Image Processing and Computer Vision]: Scene Analysis-Tracking; I.6 [Image Processing and Computer Vision]: Monte Carlo; C.5.3 [Computer System Implementation]: Microcomputers-Portable Devices (e.g., laptops, personal digital assistants)

1 INTRODUCTION

Outdoor Augmented Reality (AR) applications today rely mostly on the built-in sensors to provide localization. Todays smartphones achieve self-localization by Global Positioning System (GPS), along with a digital compass and inertial orientation sensors like gyroscope or accelerometer. Due to limited accuracy, AR applications cannot rely solely on the sensors of smartphones. Therefore, alternative methods must be used to replace or assist the sensors.

Vision-based methods for global localization are the most promising, because of their high precision in estimating the camera pose and their ability to run in real time on modern hardware [17]. In this work we apply image-based rendering to evaluate hypotheses from a particle filter and determine the most likely camera pose.

2 RELATED WORK

There are two dominant approaches to image-based localization. The first requires knowledge of the scene beforehand [6, 4, 8, 14]. In this approach, vision-based localization is solved by (a) using a collection of images or (b) a 3D model as reference. The second approach is Simultaneous Localization and Mapping (SLAM), where the camera is localized while the system builds a map of the unknown scene.

Structure from Motion (SfM) approaches enable the creation of large-scale 3D models of urban scenes. These compact scene rep-

---

[*]e-mail:chris01@sbox.tugraz.at

[†]e-mail:arth@icg.tugraz.at

[‡]e-mail:schmalstieg@tugraz.at

[§]e-mail:jventura@uccs.edu

resentations can be used for accurate image-based localization. As the scene gets larger, recognizing unique landmarks becomes more challenging. This difficulty is overcome by using sophisticated image features such as Scale-Invariant Feature Transform (SIFT) [9], but these are too expensive to compute in real-time [14, 6, 8, 18].

Reitmayr and Drummond [11, 12] present an edge-based tracking system using textured 3D building models for accurate tracking on a smartphone. They make use of the video image as well as gyroscope and measurements of gravity and magnetic field. This work mainly addresses frame-to-frame tracking, but also includes an approach for re-localization using features extracted using the FAST corner detector [13].

Aubry et al. [2] demonstrate a technique that can reliably align images of architectural sites, like drawings, paintings or historical photographs, to a 3D model of the site. To align different query inputs like drawings to a 3D model, local feature matching based on interest points, e.g., SIFT, often fails to find correspondences across paintings and photographs. Sibbing et al. [15] explore how point cloud rendering techniques can be used to create virtual views from which one can extract features that match image-based features as closely as possible.

Our approach also uses rendering of a textured model from many possible poses; however, in contrast to Reitmayr and Drummond [11, 12], we use pixel-wise cost functions instead of edge search and apply our cost functions to continuous particle filtering, rather than one-shot localization. Thus, our approach unifies localization and continuous tracking in a single method.

3 SYSTEM OVERVIEW

Our approach requires matching of a video stream from a smartphone to a virtual model. Therefore, our system uses a virtual model and sensor readings from a smartphone as input data.

The rendering of the virtual environment requires a geo-registered model of the environment and geo-registered panorama images for texturing the model.

Data collected from the smartphone includes the video stream and device pose as estimated by the non-visual sensors. The device delivers latitude and longitude from the GPS unit in the WGS84 datum and orientation as yaw, pitch and roll angles from the inertial measurement unit (IMU). In our experiments we run the particle filter algorithm on a desktop computer.

4 PARTICLE FILTER

A particle filter is a simulation-based method for tracking a system with partially observable state. We briefly review particle filters in this section. The reader is referred to Thrun et al. [16] for a more detailed review. A particle filter maintains a weighted and normalized set of sampled states, $S_t = \{\langle x_t^i, w_t^i \rangle \ i = 1, ..., N\}$, called particles p_t^i, where x_t^i is the state of the ith particle and w_t^i is its weight. The weight of a particle can be thought of as the probability that the particle's state corresponds to the true state of the system. In our case, the state is the camera pose. In our system, one iteration is processed for every new frame when it arrives. The steps of one particle filter iteration are as follows:

IEEE computer society

Figure 1: The system uses a geo-registered mesh model (left) and panorama images (middle) as input. Using projective texture mapping, both input data sources are combined to produce virtual renderings of the environment (right).

1. Each particle is propagated according to our propagation model

2. Their weights are computed by comparing rendered and real world frames

3. The top ranked particles are re-sampled to obtain a new set of equally weighted particles, which approximates the new posterior distribution

4.1 Motion model

In this discussion, we refer to the device pose delivered by the internal GPS/IMU sensors as the "sensor pose."

Each particle p_t^i is formed by perturbing a prior pose by a sample from a statistical motion model. Similar to the work of Klein and Murray [7], we sample these motions from a Gaussian noise model. For the initial step we propagate particles as follows:

$$p_{t,d}^i = c_{i,d} + \mathcal{N}(0, \sigma_d) \tag{1}$$

where p_t^i is the particle, $c_{i,d}$ the d-th dimension of the sensor pose c_i of the ith frame and σ_d the standard deviation of the noise added for that dimension. For the following re-sampling steps, c is replaced by the state of one of the most probable particles from the previous iteration.

$$p_{t,d}^{i+} = p_{t,d}^{i-} + \mathcal{N}(0, \sigma_d) \tag{2}$$

where p_t^{i+} is a particle for the current frame, p_t^{i-} is a probable particle of the previous frame, d the dimension and σ_d the standard deviation of the noise added for that dimension.

For each frame, changes in the sensor data are measured. The most probable particles p_t^{i-} are duplicated and modified with the sensor changes between the current and the previous frame.

$$p_t = p_t^{i-} + (c_i^+ - c_i^-) \tag{3}$$

where c_i^- is the sensor pose of the previous frame and c_i^+ the sensor pose of the current frame. The unmodified sensor pose is also added as a particle.

In summary, for maximum robustness, our particle re-sampling includes (a) the most likely particles from the previous iteration (b) the most likely particles, modified with changes between the current and last frame according to the sensors and (c) the unmodified sensor pose.

4.2 Calculating particle weight

To compute the weight of a particle, we compare an image rendered at the particle's pose to the current image from the device camera.

We use two different weighting approaches in order to capture color, texture and edge information.

The image sum of squared distances (SSD) method compares the rendered image to the image captured from the smartphone, with a mask applied. We mask out the part of the rendering corresponding to the sky (pixels not belonging to any scene geometry), specified as a binary mask $m_j \in \{0,1\}$. We compute the SSD for each particle p_i as follows:

$$e_I^i = \frac{\sum_j m_j \cdot ||I_j - V_{i,j}||^2}{\sum_j m_j} \tag{4}$$

where e_I^i is the error, I is the camera image, and V_j is the rendered image for particle i.

The gradient magnitude SSD method computes the average difference between the gradient magnitudes of the rendered image and the masked gradient magnitudes of the camera image as follows:

$$e_G^i = \frac{\sum_j m'_j \cdot (||G_j^I|| - ||G_{i,j}^V||)^2}{\sum_j m'_j} \tag{5}$$

where e_I^i is the error, G^I contains the gradient magnitudes of the camera image, G_i^V contains the gradient magnitudes of the rendered image for particle i, and m' is the binary mask after applying a dilation operator to avoid masking out the contours of the buildings. The gradients are computed using the Sobel operator applied to the rendered and the real world image.

The error value for each method is normalized so that

$$\sum_{i=0}^N e_I^i = 1, \quad \sum_{i=0}^N e_G^i = 1 \tag{6}$$

The weights are then calculated as

$$w_I^i = \exp(-e_I^i), \quad w_G^i = \exp(-e_G^i) \tag{7}$$

and normalized so that

$$\sum_{i=0}^N w_I^i = 1, \quad \sum_{i=0}^N w_G^i = 1 \tag{8}$$

The final weight is calculated simply as the sum of the weights from the two methods:

$$w^i = w_I^i + w_G^i \tag{9}$$

The particle with the highest combined weight w^i is considered the best estimate of the device pose, i.e., the pose to be used for AR rendering.

Before computing the error functions and weights, all images under consideration are downsampled. This helps to avoid or reduce artifacts and to improve performance.

Dimension	σ_d	Approx. range
x_{eye}, y_{eye}	5.5	up to 9 meters
x_{center}, y_{center}	0.25	up to 15 degrees
$z_{center}, x_{up}, y_{up}, z_{up}$	0.085	up to 5 degrees

Table 1: Noise parameters for the initialization step.

Dimension	σ_d	Approx. range
x_{eye}, y_{eye}	0.36	up to 60 centimeters
x_{center}, y_{center}	0.01	up to 0.5 degrees
$z_{center}, x_{up}, y_{up}, z_{up}$	0.01	up to 0.5 degrees

Table 2: Noise parameters for the update steps.

5 EXPERIMENTS

The test areas for our particle filter system are the Hauptplatz and Tummelplatz in Graz, Austria. For recording GPS, IMU data and the video stream we used an Apple iPhone 4. To process the particle filter, we used a desktop computer with an Intel Core i7-4770, 16 GB RAM and an AMD Radeon R9 280X.

5.1 Implementation notes

This section provides some details about the particle filter configuration. Each frame has a width of 100 pixels, whereas the height depends on the aspect ratio of the smartphone image. Our system is initialized with 1000 particles. The chosen noise parameters for the initial particle distribution governed by Equation 1 are given in Table 1.

In the subsequent update iterations, the three most probable particles and the sensor pose c_i are used for re-sampling. The chosen noise parameters for the particle motion model governed by Equation 2 are given in Table 2. In total, the update step uses only 20 particles. For future work we consider to use Kullback-Leibler distance (KLD)-sampling to decide if the resampling step is necessary. This approach adjusts the number of samples based on the likelihood of observations [5].

5.2 Results and discussion

We tested our system with many images and videos recorded in our test areas. Figure 2 shows that we achieve accuracy within 50 cm on a geo-referenced image. After initialization (669 ms), the system runs at 30Hz. The rate of convergence would likely be increased by using more particles in the update steps, but in our tests we used the maximum number of particles possible to achieve real-time rates with our current unoptimized implementation.

Figure 3 shows sampled frames from the test videos alongside renderings of the virtual environment, comparing the best pose from the particle filter to the uncorrected sensor pose. As can be clearly seen in these examples, our approach significantly improves the camera pose and offers much better real-virtual alignment than the raw camera pose delivered by the GPS and IMU sensors. We also found that our system is robust to image artifacts like shadows and the presence of objects that are not in the virtual environment, like cars or people. Examples of occluding objects are shown in the second row of Figure 3, where occluding people, street cars, and street carts are present in the query image.

In most cases, the rendering of the best particle closely matches the input camera image. However, in Figure 2, some jitter in the pose can be observed. We found that, because the 3D model is textured with projective texture mapping, the localization result is negatively affected if the camera's viewing angle differs greatly from the viewing angle of the images used to make the 3D model. The nature of the random sampling process in the particle filter can also cause jittering in stationary scenes, for example, when two particles have similar weights, but slightly different poses.
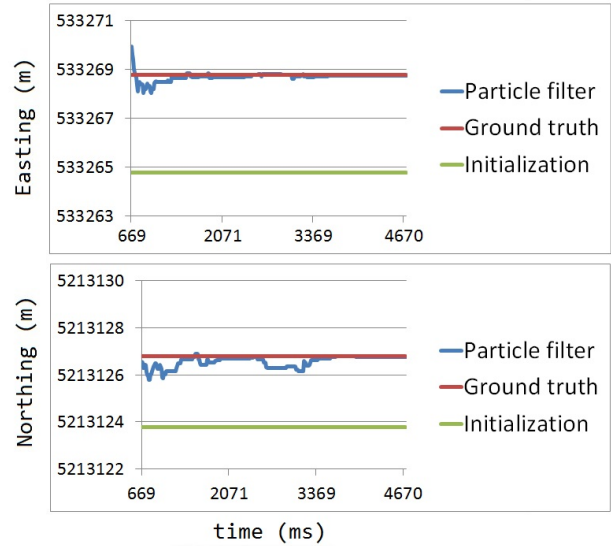

Figure 2: Result of particle filter iterations on a geo-referenced image.

Our experiments indicate that SSD is less effective if a significant amount of sky is visible, causing the number of pixels under consideration to decrease and leading to a high weight. Conversely, gradient magnitude SSD works best when parts of the building and parts of the sky are visible. This is because the highest gradients are at the contour of the buildings. Thus the two weights are complementary and it makes sense to combine them.

Although our system as tested is implemented on a desktop computer, we are confident that the approach could easily achieve real-time rates on mobile hardware. This is because most of the computation consists of either rendering of textured models with low polygon count or simple image processing operations with small filter size.

6 CONCLUSIONS AND FUTURE WORK

Our work has demonstrated an accurate outdoor localization system that runs in real time. The particle filter is flexible in its ability to adapt to different computation environments and different desired levels of performance, accuracy and robustness, by simply adjusting the number of particles and propagation model used.

Another interesting property of our system is that both localization and continuous tracking are achieved with the same method. In addition, we do not make any use of slow-to-compute feature descriptors or large descriptor databases and, instead, only require a simple textured model of the target environment. Therefore, a mobile version of the application may be feasible in the near future.

A disadvantage of the proposed system is increased jitter in stationary scenes. This condition occurs when two particles with a slightly different pose have a similar weight. One possible solution is to back-project feature points to the synthetic model in order to obtain 3D-2D matches that can be used to run a much more stable and faster tracking [1].

One avenue of future work is to improve the particle propagation model. A more accurate distribution function could provide even further performance, because fewer particles would be necessary. For example, a pedestrian motion model could be used [10]. Another improvement would be view-dependent rendering [3] to increase the accuracy of the image-based rendering and the range of the localization.

Our work hints at the possibility that image-based localization

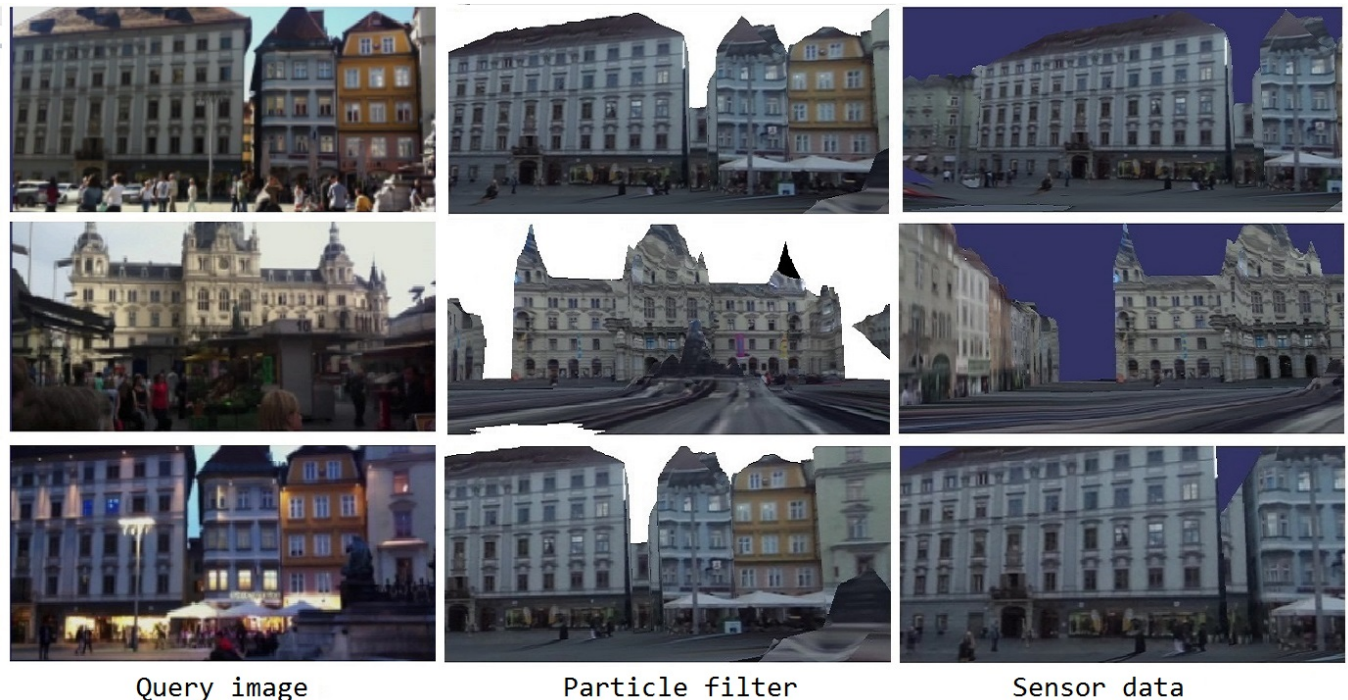| Query image | Particle filter | Sensor data |

Figure 3: The input data for a pose query is an image from the smartphone (left) and sensor data from GPS and gyroscope. The device sensors are used as an initial guess (right). Our system provides an improvement of the initially guessed camera pose (middle). Note the robustness to issues such as occluding objects (second row) and lighting (third row).

based on sparse descriptors may in the long run be replaced by dense GPU-based methods. In particular, the increasing availability of high-quality urban models created with structure-from-motion methods, supported by large geo-data providers such as Google or Microsoft, can be leveraged in GPU-based "tracking by synthesis" approaches such as the one explored in this paper.

References

[1] H. Alvarez, I. Aguinaga, and D. Borro. Providing guidance for maintenance operations using automatic markerless augmented reality system. In *Mixed and Augmented Reality (ISMAR), 2011 10th IEEE International Symposium on*, pages 181–190, Oct 2011.

[2] M. Aubry, B. C. Russell, and J. Sivic. Painting-to-3d model alignment via discriminative visual elements. *ACM Trans. Graph.*, 33(2):14:1–14:14, Apr. 2014.

[3] P. E. Debevec, Y. Yu, and G. Borshukov. Efficient View-Dependent Image-Based Rendering with Projective Texture-Mapping. *Rendering Techniques*, pages 105–116, 1998.

[4] Z. Dong, G. Zhang, J. Jia, and H. Bao. Keyframe-based real-time camera tracking. In *Computer Vision, 2009 IEEE 12th International Conference on*, pages 1538–1545, Sept 2009.

[5] D. Fox. Kld-sampling: Adaptive particle filters. In T. G. Dietterich, S. Becker, and Z. Ghahramani, editors, *NIPS*, pages 713–720. MIT Press, 2001.

[6] A. Irschara, C. Zach, J. Frahm, and H. Bischof. From structure-from-motion point clouds to fast location recognition. In *Proceedings of Computer Vision and Pattern Recognition (CVPR)*, 2009.

[7] G. Klein and D. Murray. Full-3d edge tracking with a particle filter. In *British Machine Vision Conference Proc 17th*, 2006.

[8] Y. Li, N. Snavely, and D. P. Huttenlocher. Location recognition using prioritized feature matching. In K. Daniilidis, P. Maragos, and N. Paragios, editors, *ECCV (2)*, volume 6312 of *Lecture Notes in Computer Science*, pages 791–804. Springer, 2010.

[9] D. Lowe. Distinctive image features from scale-invariant keypoints. *International Journal of Computer Vision*, 60(2):91–110, 2004.

[10] M. Quigley, D. Stavens, A. Coates, and S. Thrun. Sub-meter indoor localization in unmodified environments with inexpensive sensors. In *IROS*, pages 2039–2046. IEEE, 2010.

[11] G. Reitmayr and T. Drummond. Going out: robust model-based tracking for outdoor augmented reality. In *Mixed and Augmented Reality, 2006. ISMAR 2006. IEEE/ACM International Symposium on*, pages 109–118, Oct 2006.

[12] G. Reitmayr and T. Drummond. Initialisation for visual tracking in urban environments. In *Mixed and Augmented Reality, 2007. ISMAR 2007. 6th IEEE and ACM International Symposium on*, pages 161–172, Nov 2007.

[13] E. Rosten and T. Drummond. Fusing points and lines for high performance tracking. In *Computer Vision, 2005. ICCV 2005. Tenth IEEE International Conference on*, volume 2, pages 1508–1515 Vol. 2, Oct 2005.

[14] T. Sattler, B. Leibe, and L. Kobbelt. Fast image-based localization using direct 2d-to-3d matching. In *Proceedings of International Conference on Computer Vision (ICCV)*, 2011.

[15] D. Sibbing, T. Sattler, B. Leibe, and L. Kobbelt. Sift-realistic rendering. In *3D Vision - 3DV 2013, 2013 International Conference on*, pages 56–63, June 2013.

[16] S. Thrun, W. Burgard, and D. Fox. *Probabilistic robotics*. MIT press, 2005.

[17] J. Ventura, C. Arth, G. Reitmayr, and D. Schmalstieg. Global localization from monocular slam on a mobile phone. *IEEE Transactions on Visualization and Computer Graphics*, 20(4):531–539, 2014.

[18] J. Ventura and T. Hollerer. Wide-area scene mapping for mobile visual tracking. In *Mixed and Augmented Reality (ISMAR), 2012 IEEE International Symposium on*, pages 3–12, Nov 2012.